Paper No. 653. (quote when citing this article)
Eleventh World Conference on Earthquake Engineering
ISBN: 0 08 042822 3

SEISMIC BEHAVIOR OF HIGH STRENGTH CONCRETE SLENDER WALL UNDER HIGH AXIAL LOAD

HIDEKI KIMURA *1 and SHUNSUKE SUGANO*2

*1 Researcher, *2 Senior Chief Researcher
Takenaka Research & Development Institute,
1-5 Ohtsuka Inzai-Machi Inba-Gun Chiba, 270-13, Japan
Phone : 0476-47-1700, Fax : 0476-47-3080

ABSTRACT

Specimens using 80 MPa high strength concrete (HSC) which were simulated lowest portion of slender wall in high-rise buildings were subjected to cyclic loading under high axial load. Primary variables were concrete strength (40 and 80 MPa) and axial load level. The effect of the variables on the maximum strength and the ductility in the hysteresis loop was addressed. Specimen with concrete strength of 80 MPa showed larger deformation capacity than that with 40 MPa concrete under the same axial load. Flexural capacity of HSC walls under high axial load can be estimated by conventional equation. It would be possible to design HSC slender walls with a flexture type failure mode under high axial load and HSC can be effective for slender walls in high-rise buildings.

KEYWORDS

High strength concrete; shear wall; seismic behavior; high axial load; high-rise building; high strength steel bar; cyclic loading; reinforced concrete

INTRODUCTION

The use of high-strength concrete permits taller R/C buildings even in high seismicity countries. Structural walls in R/C buildings can provide a large stiffness and a high degree of seismic protection in terms of both damage control and prevention of collapse. However, most of R/C buildings over 25 stories in Japan are ductile moment-resisting frames, because of the analytical plainness and the limited information on the performance of high strength concrete (HSC) structural walls subjected to cyclic loading. Specimens using 80 MPa concrete which were simulated lowest portion of slender wall in high-rise buildings were tested to investigate the seismic behavior.

DETAILS OF SPECIMENS AND TEST PROCEDURE

Five specimens with barbell-shaped cross section which were simulated lowest portion of slender wall in a high-rise building were made as shown in Fig. 1. Details of specimens were given in Table 1. The size of boundary elements (columns) was 200×200 mm. Thickness of the walls was 80 mm. Height-to length ratio was 1.7 for all specimens. Concrete was cast horizontally. Silica fume was added to increase the strength for 80 MPa concrete. The cover thickness measured from outside of the perimeter ties in boundary elements and

from vertical reinforcement in a panel was 10 mm. Twelve deformed bars with nominal diameter of 10 mm (12-D10) were provided for the longitudinal reinforcement of each boundary element. High strength round bar with diameter of 6 mm and with yield strength of 800 MPa was provided for both double layered panel reinforcement and ties in boundary elements. Boundary elements were well confined by ties. The ties were closed by butt-welding and the horizontal reinforcement in a panel with 135° hooks at both ends were used. Mechanical characteristics of concrete and steel bars used were given in Table 1 and 2.

Variables were 1) concrete strength (f'c: 40 and 80 MPa), 2) axial load (N: 1800, 1300 and 800 KN), 3) yield strength of longitudinal reinforcement in boundary elements (400 and 600 MPa) and 4) tie spacing of boundary elements (50 mm and 35 mm). All specimens were subjected to repeated cycles of lateral load under constant axial compression. Cantilever type loading was used. The lateral load was applied by two actuators to the point of 2400 mm height from the base using pin connection placed at center of the specimen. Loading was controlled by displacement angle measured at 1120 mm height from the base which was considered as second floor level of actual building. Loading history employed consisted of displacement angle of one cycle of ± 0.002, 0.0033, 0.005 and 0.0075 followed by two cycles of ±0.01, 0.015, 0.02 and 0.03.

Table 1 Property of specimens

Specimen	Axial load (KN)	Boundary element			Concrete		
		Cross section (mm)	Grade of main bar	Ties spacing	f'c (MPa)	fct (MPa)	Ec (MPa)
W8N18	1,765	200×200	SD345	4-6 ϕ @50mm	72.8	2.93	3.68×10^4
W8N13	1,275	200×200	SD345	4-6 ϕ @50mm	79.0	3.78	3.90×10^4
W8N08H	785	200×200	SD590	4-6 ϕ @50mm	79.4	5.60	3.85×10^4
W4N18	1,765	200×200	SD345	4-6 ϕ @50mm	43.1	2.32	3.08×10^4
W4N18C	1,765	200×200	SD345	4-6 ϕ @35mm	42.5	2.61	2.95×10^4

f'c : Compressive strength of concrete cylinder
fct : Tensile strength of concrete cylinder
Ec : Modulus of elasticity

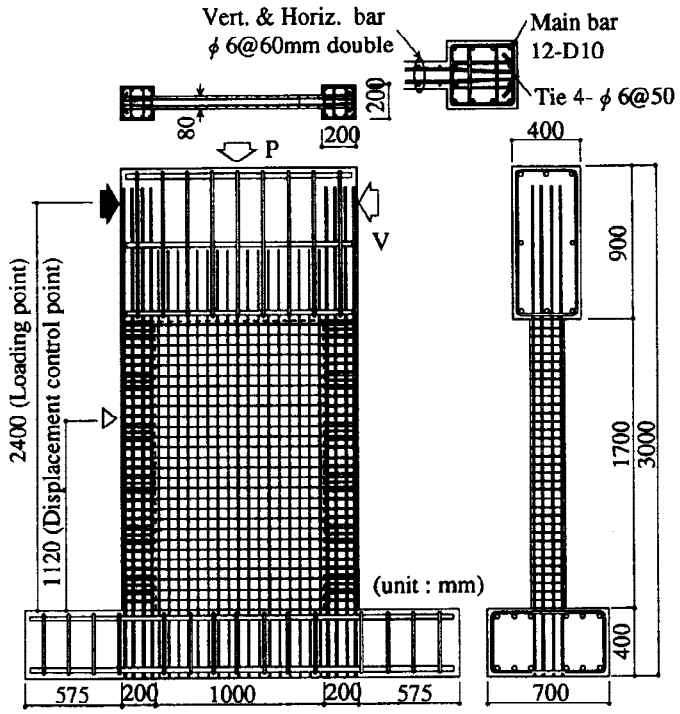

Fig. 1. Details of test specimen (W8N18)

Table 2 Mechanical characteristics of steel bars

Portion	Main bar of boundary elements	Tie & subtie	Reinforcement in panel	
Diameter (mm)	10	10	6	6
Grade*	SD590	SD345	SR785	SR785
fy (MPa)	580	385	852	849
fu (MPa)	658	654	934	926
Es (MPa)	1.96×10^5	1.85×10^5	2.03×10^5	2.02×10^5
ϵ u (%)	15.8	15.3	12.7	12.3

fy : Yield strength fu : Ultimate strength
Es : Modulus of elasticity ϵ u : Elongation
* SD : Deformed bar , SR : Round bar

TEST RESULTS AND DISCUSSION

General Behavior

Fig. 2 gives the relationships between shear force and displacement angle together with the final appearances of the specimens. Events observed during the test were shown in the same figure. Index used to evaluate a deformability was ultimate displacement angle (Ru) which was defined as the displacement angle at which 80 % of the maximum strength was sustained in the shear force versus displacement angle curve included P - Δ effect. When a large drop of the lateral load occurred during the second cycle or on the way to the larger displacement, ultimate displacement angle (Ru) was defined as the maximum displacement angle ever experienced.

Ultimate displacement angle (Ru) tends to increase as axial load decreases when the same strength concrete was used. However the specimen subjected to lowest axial load (W8N08H) exhibited smaller (Ru) than W8N13 under higher axial load of 1300 KN. This is because that W8N08H used high strength steel for main bar of boundary elements and the load drop resulted from a fracture of the high strength steel of which elongation was smaller than normal strength steel. The (Ru) of W8N18 (axial load N= 1800 KN), W8N13 (N= 1300 KN) and W8N08H (N= 800 KN) were 0.015, 0.027 and 0.024, respectively. In comparison between the specimens under the same and the highest axial load but with different concrete strength, W4N18 with 40 MPa concrete showed 10 $\sim$14 % less lateral load at the same displacement and less (Ru) of 0.01 than W8N18 with 80 MPa concrete. Specimens with 80 MPa concrete under lower axial load (130 and 80 tonf) showed stable response up to displacement angle of 0.02. The effect of the confinement of boundary elements on the shear force versus displacement angle curve was not clear (comparison between W4N18 and W4N18C).

Flexural cracks in a boundary element and shear cracks in a panel occurred in order. Specimens with 40 MPa concrete (W4N18 and W4N18C) showed vertical cracks in a panel at displacement angle ranging from 0.002 to 0.0033. However, 80 MPa concrete specimens under the same axial load did not show the vertical cracks. This is because the axial stress level in 40 MPa concrete specimens is relatively higher than that in 80 MPa concrete specimens. Failure mode of all specimens was shear compression failure at the corner of the panel base. The crushing areas expanded gradually and a large drop of load carrying capacity occurred at a certain displacement. In W8N08H subjected to lowest axial load and using high strength steel for main bar of boundary elements, fracture of the main bar and shear compression failure occurred at the same time. It should be noted that boundary elements sustained axial load after failure in all specimens.

Strain of Reinforcing Bars

Yielding of the longitudinal reinforcement in boundary elements was reached for all specimens. The vertical reinforcement in a panel exhibited yielding for 80 MPa specimens but did not for 40 MPa specimens.The horizontal reinforcement in a panel did not reach the yield strength for all specimens. High strength steel with yield strength of 840 MPa was used for panel reinforcement. The maximum strain of the horizontal reinforcement larger than 0.002 was observed in all specimens. Therefore, yielding should have occurred when normal strength steel bar was used. The lateral reinforcement in boundary elements did not reach yield strength in all specimens. Strain of the lateral reinforcement ranging from base to 150 mm height was larger than others, however, the maximum strain was 0.002 at most. The high strength lateral reinforcement did not work effectively because of a large amount of lateral reinforcement. Strain of sub-tie was almost the same value as perimeter tie. Strain of tie in W4N18C tended to be less than that of W4N18.

All specimens were failed in shear compression at the base of the panel. Confinement at the portion is main issue to increase the deformability. The location of neutral axis which was defined as the location of zero strain in a strain distribution of vertical reinforcement of the panel and main bars of the boundary elements was examined. The location of neutral axis moved to compression side of a boundary element as displacement angle increased in all specimens. In comparison of specimens with same concrete strength, neutral axis of specimen

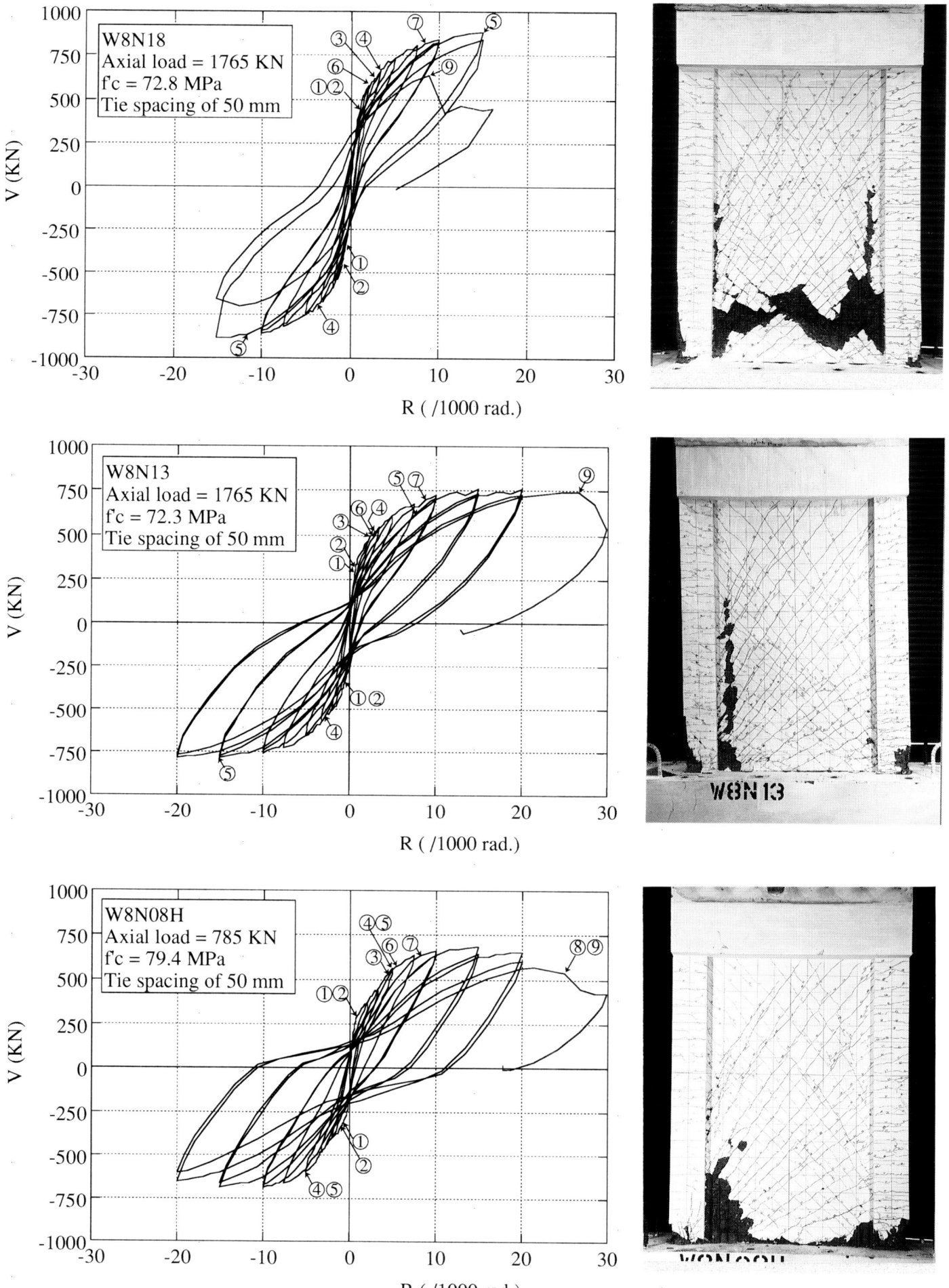

Fig. 2. Relationship between shear force and displacement angle

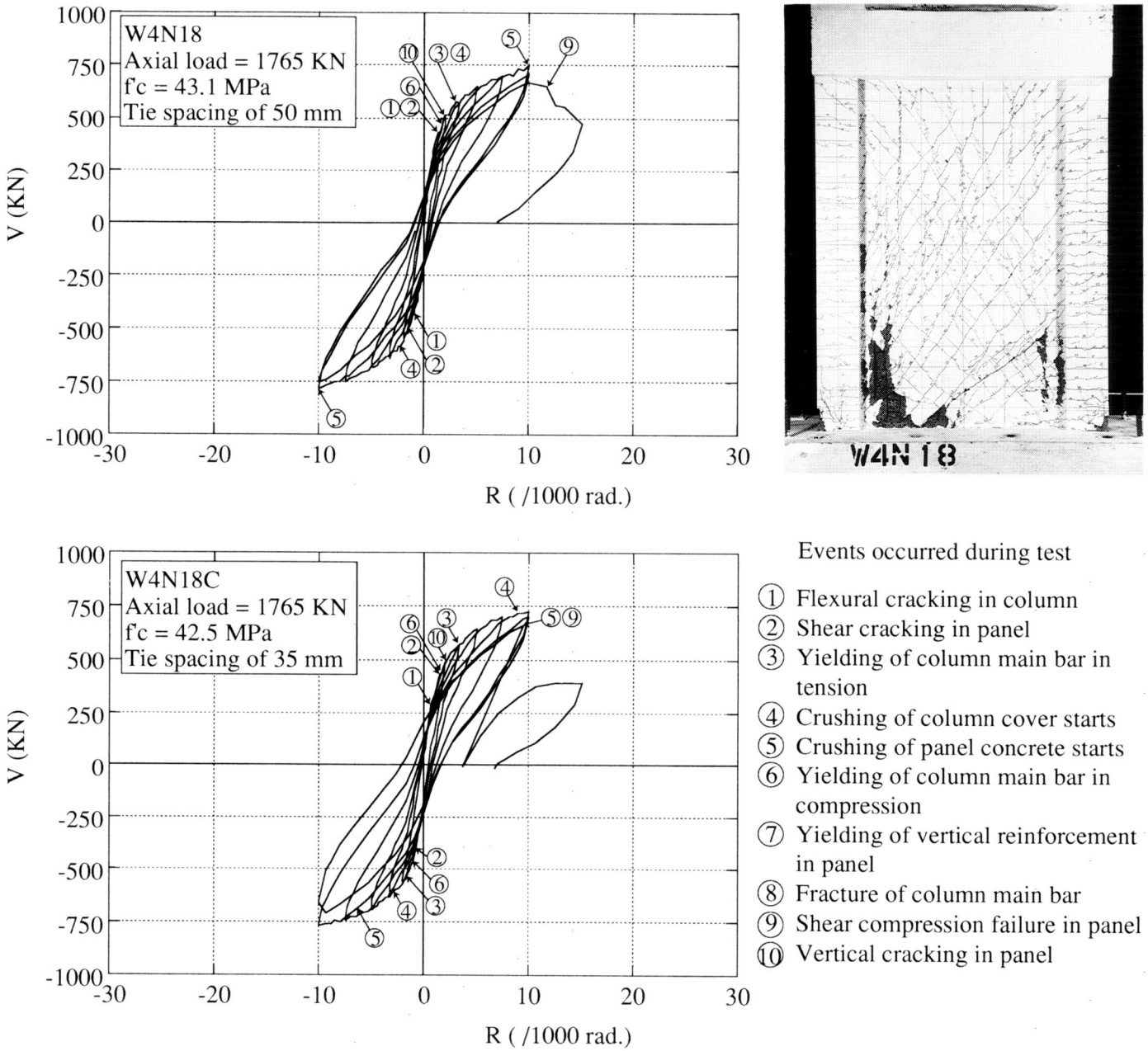

Fig. 2. Relationship between shear force and displacement angle (continued)

with higher axial load located farther from compression side. In comparison between W8N18 and W4N18 subjected to same axial load of 1800 KN but different concrete strength of 80 MPa and 40 MPa, the neutral axis of specimen with higher concrete strength at a given displacement shifted the location to compression side, because the concrete in compression area had larger value of modulus of elasticity and deteriorated less. This phenomena partly explains the larger deformability of 80 MPa concrete specimen.

Axial Shrinkage of Boundary Elements

In all of the specimens, axial shrinkages of the boundary elements were measured using displacement transducer on the middepth over the 80 mm gage length from the base. As shown in Fig. 3, a comparison of the specimens with same concrete strength of 80 MPa indicates that larger axial load gave larger axial shrinkage as expected. The axial shrinkage of W8N18 with largest axial load ranged from 0.2 to 0.4 % when displacement angle was less than 0.0075. The shrinkage increased rapidly after R = 0.0075, exceeded 1.0 % in the second cycle of R = 0.01 and reached 2.0 % at R = 0.015. The axial shrinkage of W8N08H with lowest axial load changed from positive to negative after R = 0.0075, which meant the boundary element expanded. In comparisons between specimens of different concrete strength but with the same axial load, the axial shrinkage of W4N18 progressed faster than that of W8N18. However, W4N18C with larger amount of ties in boundary

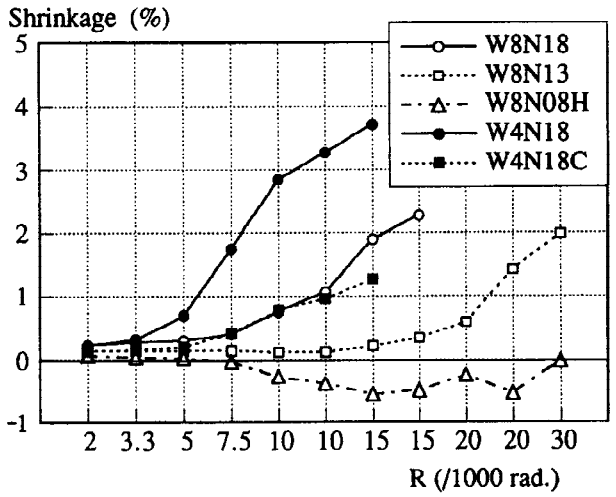

Fig. 3. Comparison of axial shrinkage of boundary element

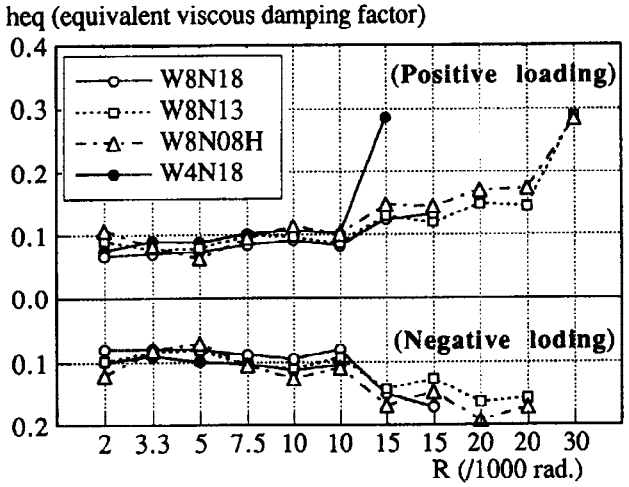

Fig. 4. Comparison of equivalent viscous damping factor

elements than W4N18 showed almost the same axial shrinkage as that of W8N18. The effect of the core confinement on the axial shrinkage was significant but the effect on the load versus displacement curve was not, because over all behavior of the walls should be determined by nature of compression areas in a panel.

Equivalent viscous damping factor

Fig. 4 shows comparisons of an equivalent viscous damping factor (heq) obtained from half cycle of each hysteresis loop. The equivalent viscous damping factor for all specimens was approximately 0.1 when the displacement angle is equal to or less than 0.01 and gradually increased after R = 0.01. The effect of tie spacing in the boundary element was not observed.

Maximum Strength

Table 3 gives relevant test results and calculated strengths. Equations used are given in footnotes. Measured maximum strengths can be substantially evaluated by equation (1) for flexural strength which is based on a flexural theory and is practically used in Japan. Ratio of measured to calculated flexural strength ranged from 1.03 to 1.31. The specimens with 40 MPa concrete exhibited less values of the ratio than those with 80 MPa concrete. To evaluate shear capacity, equations proposed in the design guideline (Architectural Institute of Japan, 1994), which was based on a plastic theory combining arch and truss shear resistance mechanisms, was used. The shear capacity decreases as the wall deformation increases because of the reduction of the strength of concrete strut due to flexural and shear cracks and/or the tensile deformation in orthogonal direction of the concrete strut. As shown in equation (5), the effective factor (ν) of the concrete strength is given as functions of both concrete strength and ultimate displacement (Ru). Modified basic value of ($\nu = 1.7\,\sigma_B^{-1/3}$) proposed in a 1987 draft of CEB-FIP Model Code (CEB, 1986) was used because the original equation apparently gave low value for high strength concrete. The (Vsu^{*1}) in Table 3 shows a calculated shear strength using a constant effective factor of concrete strut ($\nu = 1.7\,\sigma_B^{-1/3}$). In other words, the ($Vsu^{*1}$) will be used for the estimation of walls which are not allowed plastic hinges. The (ν) values for specimens with highest axial load should be larger because the (Vsu^{*1})s were less than measured maximum strengths. The (Vsu^{*2}) is a calculated shear strength using effective factor (ν : see eq.(5)) depending on the measured ultimate displacement (Ru). If the hypothesis of shear failure after flexural yielding is appropriate, the values of (Vsu^{*2}) for all specimens underestimated the measured maximum strength. However, the value might be acceptable from the view point of practical shear design for walls which are expected to form yield hinges.

Table 3 Test results and calculated strengths

Specimen	Cracking Vc (KN)		Yielding of main bar in compression		Yielding of main bar in tension		Measured maximum strength		Ultimate disp.	Calculated maximum strength		
	Flexure	shear	Vy (KN)	R (rad.)	Vy (KN)	R (rad.)	Vmax (KN)	R (rad.)	Ru (rad.)	Vmu (KN)	Vsu*1 (KN)	Vsu*2 (KN)
W8N18	433	433	567	0.0020	619	0.0027	883	0.015	0.015	706	837	657
W8N13	303	327	499	0.0027	494	0.0025	763	0.015	0.027	583	862	673
W8N08H	247	247	574	0.0053	510	0.0041	689	0.015	0.024	544	863	674
W4N18	432	432	458	0.0016	577	0.0030	753	0.010	0.010	706	704	641
W4N18C	329	433	441	0.0016	569	0.0033	731	0.010	0.010	706	701	638

(Values in this table are those observed in positive loading)

Ru : Displacement at which 80% of the maximum strength was sustained or sudden failure occurred
Vmu : Flexural strength
Vsu*1 : Shear strength calculated using constant effective factor of $\nu = 1.7\,\sigma_B^{-\frac{1}{3}}$
Vsu*2 : Shear strength calculated using effective factor (ν) according to the measured ultimate displacement (Ru) → eq.(5)

$$Vmu = (At\,\sigma_y\,lw + 0.5\,Aw\,\sigma_{wy}\,lw + 0.5\,N\,lw)/\,ho \qquad \text{---------- (1)}$$

where, At , σ_y : total area and yield strength of longitudinal tension bars in a boundary element (mm², MPa)
Aw , σ_{wy} : total area and yield strength of longitudinal bars in panel (mm², MPa)
lw : depth of shear wall measured from center to center of boundary element (mm)
N : axial load (N)
ho : wall height (shear span) (mm)

$$Vsu = tw\,lwb\,ps\,\sigma_{sy}\cot\phi + (1-\beta)\,tw\,lwa\,\nu\,\sigma_B\,\frac{\tan\theta}{2} \qquad \text{---------- (2)}$$

$$\tan\theta = \sqrt{\left(\frac{hw}{lw}\right)^2 + 1} - \frac{hw}{lw} \qquad \text{---------- (3)}$$

$$\beta = \frac{(1+\cot^2\phi)\,ps\,\sigma_{sy}}{\nu\,\sigma_B} \qquad \text{---------- (4)}$$

$$\begin{aligned} \nu &= 1.7\,\sigma_B^{-\frac{1}{3}} && (\text{when } Ru < 0.005) \\ &= (1.2 - 40\,Ru)\times 1.7\,\sigma_B^{-\frac{1}{3}} && (\text{when } 0.005 \leqq Ru < 0.02) \\ &= 0.4\times\sigma_B^{-\frac{1}{3}} && (\text{when } 0.02 \leqq Ru) \end{aligned} \qquad \text{------- (5)}$$

where, tw : thickness of wall panel (mm) , hw : height of wall (mm) , lwb =lw
lwa : total depth of shear wall including boundary columns
ps : ratio of horizontal shear reinforcement in wall panel (MPa)
σ_{sy} : yield strength of horizontal shear reinforcement in wall panel (MPa)
σ_B : compressive strength of concrete (MPa)
ϕ : angle of compressive strut in truss mechanism (assumed as $\cot\phi = 1.5$)
β : angle of compressive strut of arch mechanism

Deformation capacity

Considering the deformation capacity of shear wall, the effects of axial load, shear stress level and redundancy of shear capacity were investigated. The ratio of the axial stress in a core of the boundary element, when the wall reached flexural strength, to concrete compressive strength (K) was used to evaluate the effect of axial load. Following index (K) was used. $K = (N + A_{ws}\cdot f_{sy}) / (A_{core}\cdot f'c)$ where N = axial load, A_{ws} =total area of vertical reinforcement in a panel, f_{sy}=yield strength of the reinforcement, A_{core}=area of core in boundary element ($=Bc^2$: Bc is outside to outside distance of a perimeter tie) and f'c = compressive strength of cylinder concrete. Fig. 5 shows relationship between the ultimate displacement (Ru) and the (K). The (Ru) decreases as the (K) increases. Design guideline (AIJ, 1994) says that the ultimate displacement of 0.02 would be obtained when the (K) value is less than 0.67. The result supports the comment, however, other criteria should be needed because the ultimate displacement was determined by a crush of concrete at the base of the panel. Fig.6 and 7 plot (Ru) as functions of attained shear stress normalized by concrete strength (f'c) and redundancy of

shear capacity which was evaluated by the ratio of calculated shear capacity (Vsu^{*1}) to calculated flexural capacity (Vmu) in the Table 3. The lower the shear stress level, the larger was the ultimate displacement. And the specimen which has larger redundancy against shear exhibited larger ultimate displacement. These tendencies had been observed in specimens with lower strength concrete. More data of high strength concrete wall will be needed for the quantitative evaluation of the deformability.

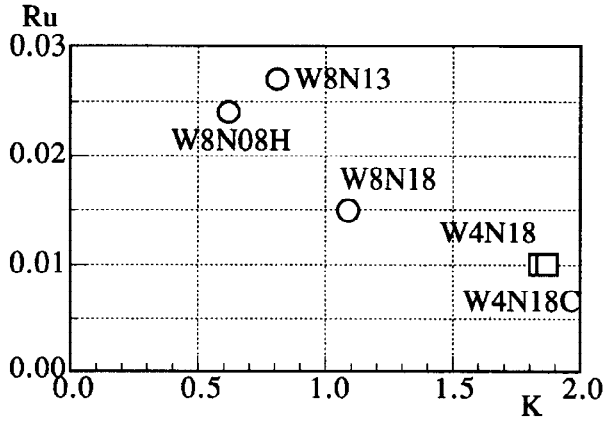

[Definition of index (K)]

$K = (N + Aws \cdot fsy) / (Acore \cdot f'c)$

N = axial load,

Aws = total area of vertical reinforcement in a panel

fsy = yield strength of the reinforcement

Acore= area of core in boundary element

f'c = compressive strength of cylinder concrete.

Fig. 5. Effect of axial load in terms of (K) factor on the ultimate displacement angle (Ru)

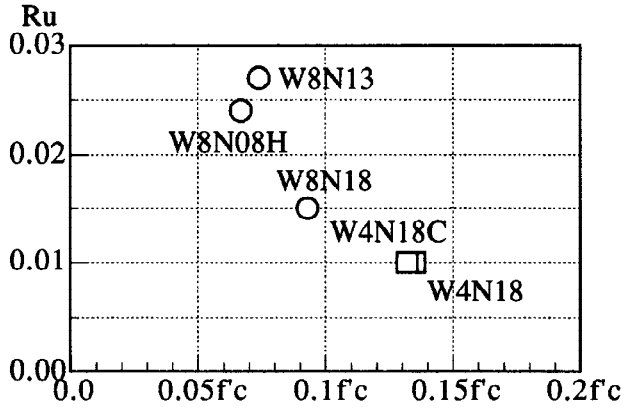

Fig. 6. Effect of shear stress normalized by concrete strength (f'c) on (Ru)

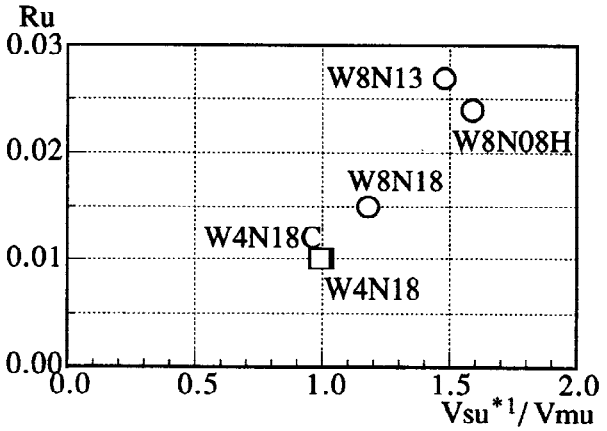

Fig. 7. Effect of redundancy of shear capacity on (Ru)

CONCLUSIONS

The following conclusions were drawn based on this study:

1)Specimen with concrete strength of 80 MPa showed larger deformation capacity than that with 40 MPa concrete under the same axial load. HSC can be effective for slender walls in high-rise buildings of which axial load is high.

2)It would be possible to design HSC slender walls with a flexture type failure mode under high axial load.

3)Flexural capacity of HSC walls can be estimated by conventional equation, even under high axial load.

4)Walls with well-confined boundary elements exhibited enough deformability after yielding up to the deformation level of web-crushing and the walls were able to sustain axial load after the failure. To prevent or delay the web crushing will be main issue to increase a deformability of the walls.

REFERENCES

Architectural Institute of Japan (AIJ) (1994). *AIJ structural design guidelines for reinforced concrete buildings based on ultimate strength concept* (in English). AIJ, Tokyo.

Comite Euro-International du Beton (CEB) (1986). *CEB-FIP Model Code (1987 draft).* CEB, Lausanne.